"Hot Electron" Photo-Charging and Electrochemical Discharge Kinetics of Silver Nanocrystals

Peter L. Redmond* and Louis E. Brus

Chemistry Department, Columbia University, New York, New York 10027

Received: May 30, 2007; In Final Form: August 3, 2007

Chronopotentiometry and chronoammperometry methods are used to study the photocharging and electrochemical discharging of Ag nanocrystals on indium tin oxide (ITO) substrates. The photocharging is initiated by Ag plasmon electronic excitation, which causes the oxidation of surface-bound citrate ions. In aqueous citrate solution, the particles discharge by reducing hydrogen. When silver ions are introduced, silver reduction increases the rate of discharge. The electrochemical kinetics is modeled quantitatively using the Butler−Volmer equation. The capacitance of the particle electrode is experimentally determined to be $\sim 2.22 \times 10^{-4}$ C/V. We conclude that high-quantum-yield surface photochemistry and photocharging is possible for well-formed nanocrystals.

Introduction

The plasmon excited electronic state in noble-metal nanocrystals is formally represented as a superposition of many low-energy electron−hole pairs. An excited plasmon, created by coherent short pulse excitation, dephases (via Landau Damping) within femtoseconds, producing one or a few higher-energy electron−hole pairs.[1−7] These higher-energy electron−hole pairs are directly created optically if a spectrally narrow cw laser is used to excite the Ag nanocrystal, as in our present experiment.[8] The excited-state electronic polarization corresponding to these directly excited "hot" carriers creates enhanced Mie scattering and the local field SERS effect. Through subsequent scattering, these hot electrons and holes thermalize and relax to the Fermi level.[9−11] Because of the extremely short lifetime of the hot carriers, optical charge-transfer reactions seem improbable. Nonetheless, several reports have found surface photochemistry caused by low-intensity (one-photon) excitation of the Ag plasmon resonance.[12−18] In related electrochemical experiments, low-intensity irradiation of rough Ag electrodes at plasmon wavelengths creates strong hot electron photoemission currents.[19−22] In high-vacuum surface science, hot Ag photoexcited electrons cause decomposition of physisorbed CCl_4 on Ag (111).[23]

In an effort to understand photocatalyzed colloidal Ag prism growth experiments, we recently reported (hereafter RWB) the electrochemical photovoltage and photocurrent response of Ag nanocrystals on ITO electrodes in sodium citrate solutions.[24] We discovered that exciting the Ag nanocrystals on the plasmon absorption causes surface-bound citrates to oxidize, thus photocharging the Ag nanocrystal. Citrate itself does not absorb visible light. We hypothesized that citrate ejects CO_2 in a decarboxylation reaction, causing irreversible electron donation into the Ag nanocrystal. In the literature, organic-acid decarboxylation following ultraviolet electronic excitation, and electrochemical decarboxylation at oxidizing potentials on metallic electrodes, are standard synthetic methods.[25,26] In 1978, Kraeutler and Bard found that ultraviolet photoexcitation of colloidal TiO_2 particles caused the decarboxylation of adsorbed carboxylic acids.[27,28] In TiO_2, photogenerated holes at energies near the valence-band edge are strong oxidizing agents. They suggested that decarboxylation occurs through the photo-Kolbe reaction shown below, causing donation of electrons into TiO_2.

$$CH_3CO_2^- + h_{vb}^+ \rightarrow CH_3CO_2\cdot \rightarrow CH_3\cdot + CO_2 \qquad (1)$$

Our system, although analogous to Kraeutler's, is remarkable and novel in that metallic electron−hole pairs are extremely short-lived compared to thermalized electron−hole pairs in TiO_2.

Once the electron has been irreversibly transferred, it remains on the now negatively charged particle until it is discharged through thermal electrochemical charge transfer. Under CW irradiation, the particles reach a steady-state cathodic potential shift defined by the equilibration of the photochemical charging rate and electrochemical discharging rate. This paper quantitatively models the kinetic response of silver particle electrodes under visible irradiation. The nanocrystals are in electrical contact with the ITO electrode surface; charge can tunnel to the electrode, establishing electrical equilibrium. We measure photovoltage under open-circuit conditions. With no current flowing, we assume that the electrode potential set by the potentiostat on the ITO equals the photostationary potential on the Ag nanocrystals. The capacitance and net charge we measure refers to charge storage on the nanocrystals, not on the combined electrode/nanocrystal system.

Experimental Section

Photoelectrochemical methods were described previously in RWB. Briefly, a platinum foil was the counter electrode and a gold wire served as a pseudo-reference electrode. A gold pseudoreference was used to avoid leaking anions from standard reference electrodes. The pseudoreference was measured against a mercury sulfate electrode and found to be stabile in the solutions we used. A 3 cm^2 area working silver nanoparticle/ITO electrode was used. All photovoltage solutions were bubbled with N_2 for 20 min to remove oxygen, and experiments were run under a blanket of nitrogen. Chronopotentiometric measurements were performed with zero net current (open circuit). Chronoamperometric measurements were performed at

* Corresponding author. E-mail: plr2001@columbia.edu.

10.1021/jp0741859 CCC: $37.00
Published on Web 09/19/2007

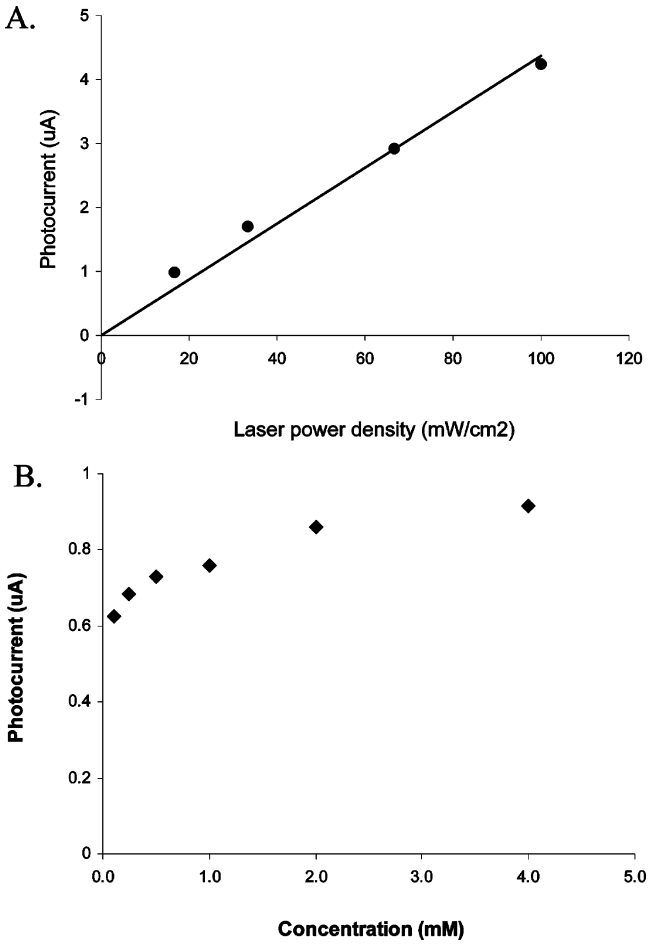

Figure 1. (A) Plot of the closed-circuit photocurrent of a silver particle electrode in 500 uM sodium citrate solution and 0.1 potassium nitrate plotted as a function of laser-power density at 488 nm. The black line shows the best-fit line. (B) Plot of the closed-circuit photocurrent of a particle electrode as a function of citrate concentration in 0.1 M potassium nitrate solution. The laser-power density was kept low (17 mW/cm^2) to make sure the reaction did not become diffusion-limited.

the rest potential of the particle electrode (closed circuit) unless otherwise stated. All photoelectrochemical experiments were run with 488-nm laser illumination.[29] No photocurrent or photovoltage shift was observed for bare ITO in solution with 500 uM sodium citrate and 0.1 M potassium nitrate. The N_2 purged solution of 500 uM sodium citrate, 250 uM silver nitrate, and 0.1 M potassium nitrate was found to have a pH of 6.57.

Results

Figure 1A shows a graph of closed-circuit photocurrent of a silver particle electrode in 500 uM sodium citrate solution plotted as a function of laser-power density. This graph shows that the current is linear with light intensity, without a sign of saturation due to possible consumption of citrate. Figure 1B is a plot of the closed-circuit photocurrent (at 17 mW/cm^2), as a function of citrate concentration in 0.1 M potassium nitrate solution. The photocurrent is a weak function of the citrate concentration (i.e., zero order). Figure 2 shows the closed-circuit photocurrent as a function of electrode potential. As the potential becomes more negative, the photocurrent decreases. This suggests lower saturation citrate coverage for more-negative Ag surfaces.

Figure 3A is a plot of the open-circuit potential versus time for a silver particle electrode before, during, and after laser irradiation in a solution of 500 uM sodium citrate and 0.1 M potassium nitrate. The potential reaches a photostationary state under laser irradiation. Figure 3B shows a plot of the equilibrium shift from rest potential of the silver particle electrodes as a

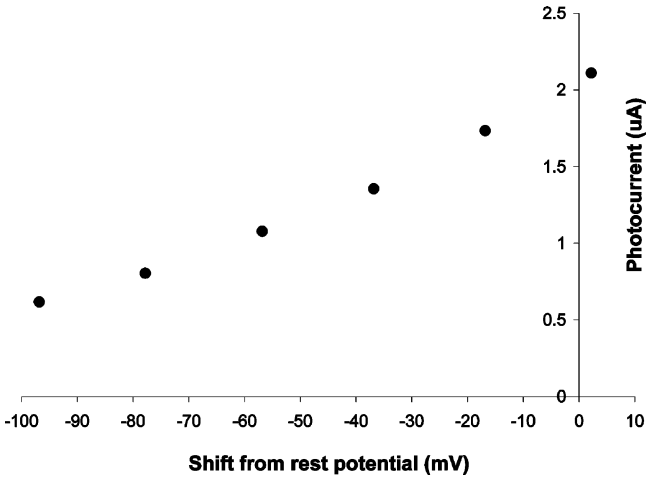

Figure 2. Plot of the closed-circuit photocurrent of a silver particle electrode in 500 uM sodium citrate solution and 0.1 potassium nitrate plotted as a function of shift from rest potential. The potential was swept at a rate of 5 mV/s, and the laser-power density was 66.7 mW/cm^2. The photocurrent is reversibly lost as the potential becomes more negative.

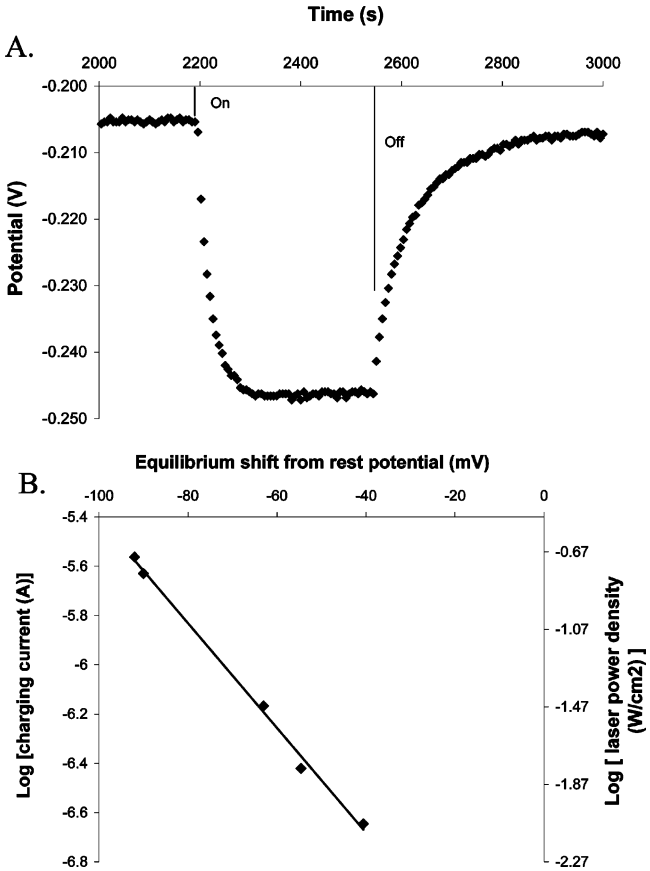

Figure 3. (A) Plot of open circuit potential vs time for a silver particle electrode before, during, and after laser irradiation in a solution of 500 uM sodium citrate and 0.1 M potassium nitrate. On and off refer to the sample under irradiation (on) and the sample in the dark (off). (B) Plot of the equilibrium shift from the rest potential of the silver particle electrodes as a function of laser-power density and charging current in a solution of 500 uM sodium citrate and 0.1 M potassium nitrate. The charging current was calculated from the curves in Figures 1 and 2 as described in the discussion.

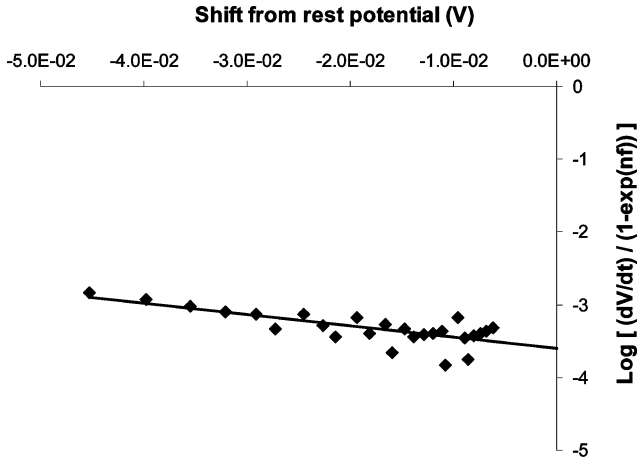

Figure 4. Plot of $dV/dt(1 - e^{fn})^{-1}$ vs η for the decay of a silver particle electrode in 500 uM sodium citrate and 0.1 M potassium nitrate.

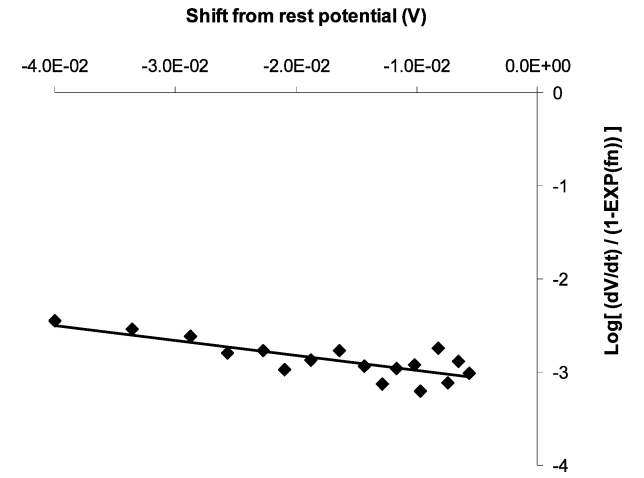

Figure 5. Plot of $dV/dt(1 - e^{fn})^{-1}$ vs η for the decay of a silver particle electrode in 250 uM silver nitrate, 500 uM sodium citrate, and 0.1 M potassium nitrate.

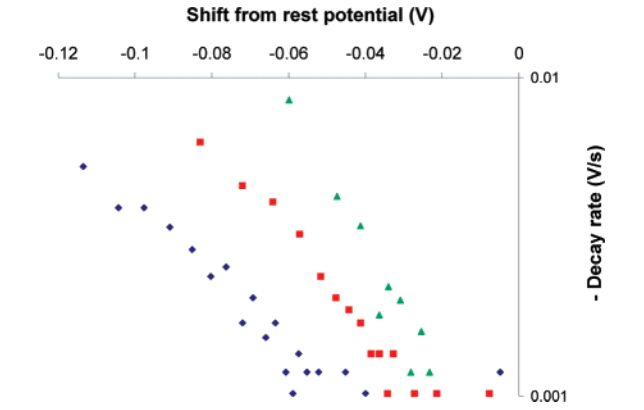

Figure 6. Semilog plot of the instantaneous decay rate as a function of potential. The blue diamonds are with 62.5 uM, the red squares are with 125 uM, and the green triangles are with 250 uM silver nitrate. Each solution contained the normal 500 uM sodium citrate and 0.1 M potassium nitrate. The graphs are cutoff at the point where digitization by the potentiostat becomes significant.

function of laser-power density and charging current in a solution of 500 uM sodium citrate and 0.1 M potassium nitrate.

As described in the Analysis section below, the potential decay is plotted in Figures 4 and 5 with and without silver nitrate. Figure 6 is the instantaneous voltage decay as a function of shift from rest potential for different concentrations of silver nitrate. The decay rate is a function of the silver ion concentration. The experimental linear dependence of the instantaneous decay rate on the silver ion concentration at different potentials is plotted in Figure 7. Figure 8 shows a CV of the two electrodes in solutions of 500 uM sodium citrate and 0.1 M potassium nitrate with and without silver nitrate.

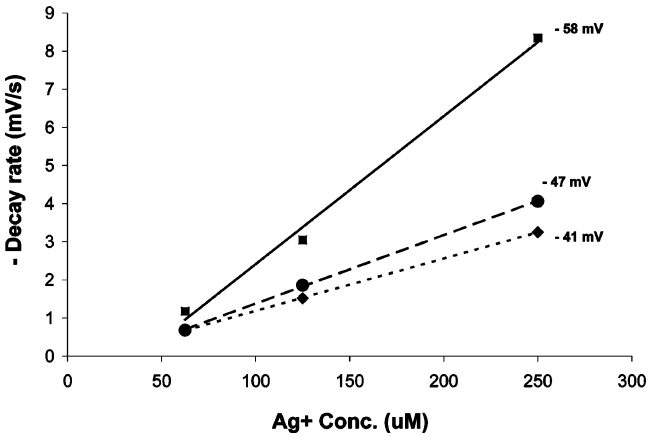

Figure 7. Plot of the instantaneous decay rate vs silver ion concentration at different potentials. This is the same data shown in Figure 6.

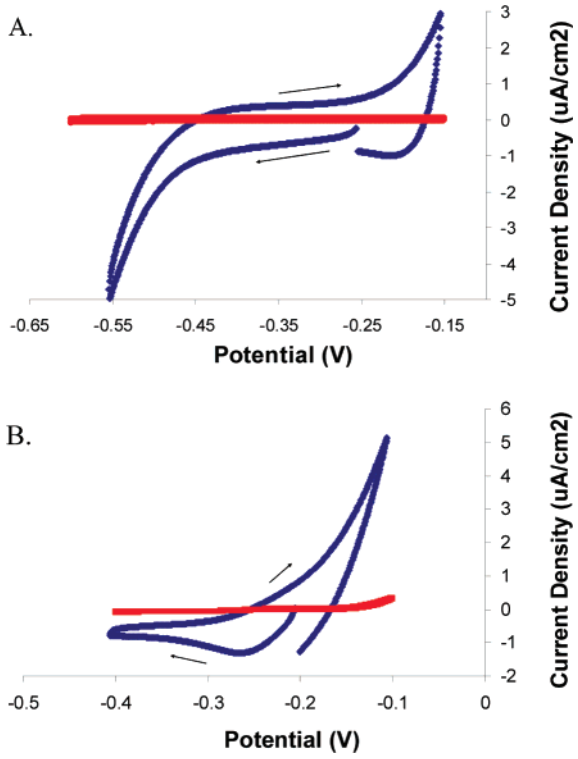

Figure 8. Cyclic voltammograms of naked ITO (red curve) and thermally untreated silver-coated ITO (blue curve) in 0.1 M potassium nitrate and 500 uM sodium citrate. A has no silver nitrate. B has 250 uM silver nitrate.

Analysis

The linear photocurrent in Figure 1A is generated on the Ag nanocrystals; we showed in RWB that there is no photocurrent without the Ag nanocrystals. Figure 1B shows a weak dependence of the photocurrent on citrate concentration. We conclude that we essentially have saturation coverage of citrate on the Ag particles at the operating rest potential. Strong adsorption and essentially complete coverage is expected from the fact that citrate is an excellent electrostatic stabilizer for colloidal Ag nanocrystals.[30,31] The absence of saturation in Figure 1A also

implies that current is not limited by possibly slow exchange of surface citrate with aqueous citrate. In Figure 2, the photocurrent is reduced at more-negative potentials presumably due to desorption of the negatively charged citrate ions.

In Figure 3A, when the laser is on, the potential shifts to negative because of the donation of electrons into the particles. When the laser is turned off, the potential decays back to the original rest potential by discharging stored electrons. The particle electrode is thought to discharge through electrochemical reduction of H_2O, as originally described by Henglein and Lillie for charged aqueous Ag nanocrystals.[32] A photostationary potential occurs under irradiation when the rate of charging is equal to the rate of discharging. Equation 2 defines the photostationary potential shift as a function of photocharging rate (J) using the Butler−Volmer equation to describe the electrochemical discharge of the electrode:[33]

$$dQ/dt = 0 = i_o[e^{-\alpha f\eta} - e^{(1-\alpha)f\eta}] - J \qquad (2)$$

Q is the net photocharge on the nanocrystals on our 3 cm^2 electrode, i_o is the exchange current, α is the transfer coefficient, $f = F/RT$, F is Faraday's constant, R is the gas constant, T is temperature, $\eta = V - V_{eq}$, V is the photostationary potential, V_{eq} is the rest potential of the electrode in the dark, and J is the photochemical charging rate. Figure 1 shows that the light-induced current is a one-photon, linear function of laser intensity. Figure 2 shows that the light-induced charge transfer of electrons into the particles is a function of the potential of the particle electrode. The data in Figures 1 and 2 were combined to describe the charging rate as a function of laser-power density. This allows us to add the charging current axis to Figure 3.

The decay of the potential in Figure 3A can be described by rearranging eq 1 with $J = 0$.

$$C\frac{dV}{dt} = i_o[e^{-\alpha f\eta} - e^{(1-\alpha)f\eta}] \qquad (3)$$

The photocharge Q on the nanocrystals is $C(V-V_{eq})$, where V_{eq} is the initial rest potential in the dark and C is the total nanoparticle capacitance. Rearrangement followed by taking the logarithm yields

$$\log\left[\frac{dV}{dt}[1 - e^{f\eta}]^{-1}\right] = \log\left[\frac{i_o}{C}\right] - \frac{\alpha f\eta}{2.3} \qquad (4)$$

Equation 4 shows that in a semilog plot of $dV/dt(1 - e^{f\eta})^{-1}$ versus η the slope is $-\alpha f/2.3$ and the intercept is $\log[i_o/C]$.[34] Figure 4 shows this plot for the decay of the potential in 500 uM citrate solution and with 0.1 M potassium nitrate. The best-fit linear line in Figure 4 has a slope of −15.6 and a y-axis intercept of −3.6. From this, we calculate a transfer coefficient of 0.92 and a capacitance of $4 \times 10^3 i_o$. Using the Butler−Volmer equation again, the intercept of the best-fit line in Figure 3 is equal to $\log[i_o] = -7.26$. From this, we get an exchange current of 5.5×10^{-8} C/s and a capacitance of 2.2×10^{-4} C/V. Literature values for the transfer coefficient of hydrogen reduction on crystalline silver without adsorbed citrate are about 0.4.[35]

We compare the experimentally determined total nanocrystal capacitance with simplified theoretical models. The silver particle electrode has a particle density of $\sim 3.8 \times 10^{-4}$ particles/nm^2. We calculate the Debye length in a 0.1 M potassium nitrate solution to be about 30.4 nm, making the area required by each particle such that it cannot "feel" the potential of its neighbor 2.9×10^3 nm^2. This corresponds to a particle density of 3.45×10^{-4} nm^2/particle. Therefore, as a rough approximation for the capacitance we model the interacting particles as a solid Ag sheet of thickness 2.5 nm (i.e., the thermal evaporation thickness). A simple calculation shows that the potential at the surface of an infinite slab of thickness d is

$$V[x = d/2] = \frac{-\rho(d/2)^2}{2\epsilon} \qquad (5)$$

where ρ is the charge density (Q/cm^3) and ϵ is the permittivity of the solvent. Applying the Gaussian pillbox method, we find the capacitance to be $C = (Q/V) = -(8A\epsilon)/d$ where A is the area of the electrode and Q is the total charge on the silver slab. Using $A = 3$ cm^2, $\epsilon = 80\epsilon_o$, and $d = 2.5$ nm, the capacitance is calculated to be 6.8×10^{-4} C/V. This is in rough agreement with the experimentally determined capacitance of 2.2×10^{-4} C/V.

Alternatively, the nanocrystal capacitance can be estimated as a group of noninteracting spheres. The capacitance of the nanoparticles is then $C = 4\pi\epsilon RN$, where R is the particle radius and N is the total number of particles on the electrode. In water with a radius of 25 nm, the capacitance is 2.5×10^{-5} C/V (with $N = 1.14 \times 10^{11}$ for our 3 cm^2 electrode). We ignore here the actual dielectric environment on the ITO surface. The experimentally determined capacitance lies between the predictions of these two oversimplified models.

Using the experimental capacitance, we can consider the case of the particle electrode discharge with Ag^+ in solution, shown in Figure 4 of RWB. We assume that the potential discharge of the particle electrode is described by the Butler−Volmer equation just as before with hydrogen reduction. The silver particle rest potential is about −205 mV versus Au wire in citrate solution. With 250 uM silver nitrate added, the rest potential becomes −137 mV versus Au wire. Accounting for the pseudoreference electrode,[36] the difference between rest potentials is about 90 mV. This tells us that silver ions in solution will be reduced at a potential 90 mV positive of where hydrogen reduction takes place. Therefore, in this analysis we need only consider electron discharge through silver reduction. Figure 5 shows a plot for the decay of the potential in a solution of 250 uM silver nitrate, 500 uM citrate, and 0.1 M potassium nitrate. The best-fit linear line in Figure 5 has a slope of −16.26 and a y-axis intercept of −3.14. This gives a transfer coefficient of 0.96 and an exchange current of 1.6×10^{-7} C/s. Transfer coefficient literature values for Ag^+/Ag range from 0.5 to 0.8 with out adsorbed citrate.[37] The low value of the exchange current for Ag+ reduction shows the effect of citrate capping in passivating the surface; the reduction is quite slow. The high value of the transfer coefficient shows that solvated Ag^+ is on the outside of the surface citrate double layer.

According to the temperature-dependent Butler−Volmer equation, the exchange current (i_o) should be linearly dependent on the silver ion concentration as can be seen in eq 6.[38−40]

$$\frac{i_o}{A} = nF\left(\frac{kT}{h}\right)a_o \exp[(-\Delta G^{act} + \alpha F V_{eq})/RT] \qquad (6)$$

This equation shows that the Butler−Volmer model is a type of absolute rate theory. Here A is the area of the electrode in square centimeters, n is the number of electrons transferred in the reduction, k is Boltzman's constant (1.38×10^{-23} J/K), h is Plank's constant (6.626×10^{-34} J/s), ΔG^{act} is the standard Gibbs free energy of activation in Joules per mole, and a_o is the molar activity of the oxidized species (Ag^+) in units of moles per square centimeter. Thus, the instantaneous voltage decay

TABLE 1: Electron Discharge Rate as a Function of Shift from Rest Potential as Calculated from the Butler−Volmer Fits[a]

shift from rest potential (mV)	e^-/particle with $r = 25$ nm	discharge rate: e/(s·particle) hydrogen reduction	discharge rate: e/(s·particle) silver reduction
−300 mV	411	1.4×10^5	6.5×10^5
−30 mV	41	6.1	18.4
−3 mV	4	0.4	1.1

[a] The calculated values assume a solution of 250 uM silver nitrate, 500 uM sodium citrate, and 0.1 M potassium nitrate.

rate at any potential should be linearly dependent on the silver ion concentration. The experimental linear dependence of the decay rate on silver ion concentration is shown in Figure 7.

In our analysis so far, we have assumed that the photovoltage decays by charge transfer on the Ag nanocrystal surfaces, and not on the ITO. To test the relative contributions of the particles and the ITO to the charge-transfer rate, we took cyclic voltammograms with naked ITO and silver film/ITO electrodes (Figure 8). The silver film/ITO electrodes were prepared by thermally evaporating 5 nm of silver onto an ITO-coated glass slide. This electrode was not heat-treated, leaving a continuous film, allowing us to better estimate the area of the electrode. Figure 8A does not have any silver nitrate; the reduction of hydrogen causes the negative current on the silver electrode while very little current flows on the naked ITO. Figure 8B has 250 uM silver nitrate and shows a reduction peak for silver at −270 mV versus Au wire while ITO shows almost no reductive current. At a shift of −50 mV from rest potential, hydrogen reduction current is 120 times larger on silver than on ITO and the silver reduction is 13 times larger on silver than ITO. From this, we conclude that the particle electrode discharges primarily through surface reactions on the silver particles.

Figure 4 of RWB shows that the photovoltage decay is nonexponential when the laser is turned off.[24] In the Butler−Volmer equation, the rate of electron transfer is strongly nonlinear in the excess voltage, for fixed Ag^+ concentration. The figure S1 $I-V$ curve shows that below about −80 mV photovotage (i.e., our photovoltage range in the presence of Ag^+), the charge-transfer rate is limited by the time required for an electron to tunnel from the particle to Ag^+ solution. Table 1 shows the electron-transfer rate per particle as a function of shift from rest potential as calculated from the Butler−Volmer fits. The calculated values in Table 1 assume a solution of 250 uM silver nitrate, 500 uM sodium citrate, and 0.1 M potassium nitrate. The number of electrons on each particle was calculated from the isolated sphere capacitance model. The decays are quite slow: with about 40 photoelectrons on one nanocrystal, the H-reduction decay rate is only about 6 electrons/s.

Discussion: High Yield of Surface Photochemistry?

The photocurrent at the rest potential in Figure 2 is about 2 uA. Using the dry electrode optical extinction coefficient, we find that this corresponds to a current to photon-scattering ratio ("Quantum Yield", QY) of about 6.3×10^{-5} e^-/photon. This average value over the 3 cm^2 electrode is 2 orders of magnitude lower than our previous estimate in RWB. The prior estimate was based upon individual nanocrystal photocatalytic growth rates, for colloidal silver particles on insulating Formvar/carbon TEM grids.[41] The bulk measured QY in present paper is much too low to account for the growth seen in RWB. The discrepancy in QYs may be due to the nature of the particle/ITO contact. On the ITO surface, if there is poor electrical contact between the Ag nanocrystal and ITO, then the quantum yield for the few well-contacted nanocrystals would be higher but the bulk measurement would show a low QY.[42] Another possible reason for the low bulk QY is that all of the particles are in electrical contact with the ITO but only a few of them are photoactive.[43] Finally, the citrate reduced particles used in RWB are of higher crystalline quality than the evaporated Ag particles used here. This should have a great effect on the QY. This point is discussed further in the following paragraph.

What is the highest possible quantum yield for a single Ag particle? In small molecules, photophysical quantum yields are an intrinsic property. This is not the case for nanocrystal samples where structure and surface molecular coverage vary from one nanocrystal to the next. It is necessary to minimize the internal decay rate of the hot carriers (excited electronic polarization) to the rate of perfectly crystalline bulk Ag in order to maximize the charge-transfer quantum yield (and also the SERS local field enhancement). When the plasmon is calculated using the bulk Ag ac dielectric constant, a perfectly crystalline particle is assumed. Actual colloidal particles have numerous defects, and typical plasmon spectra are broader that the theoretical ideal. In this connection, Gutierrez and Henglein showed that unusually narrow plasmon resonances were observed for slow, reversible Ag^+ reduction making essentially perfect nanocrystals.[44] In our ITO experiment, TEM and SEM examination of the nanocrystals, made by thermal evaporation followed by annealing, shows they are not as crystalline and well-formed as the Lee and Meisel (citrate reduction method) Ag particles used in the prior RWB quantum yield estimate. A lower degree of crystallinity for the evaporated particles would increase the hot-carrier decay rate and lower the quantum yield. Also, the close physical contact of the Ag with the ITO may provide an additional decay pathway for excited electron−hole pairs,[45] and prevent citrate absorption over the entire nanocrystal surface.

Theoretically, for well-formed Ag nanocrystals of a few nanometers size, surface scattering dominates relaxation. The relaxation rate scales as radius R^{-1} (ref 1); also, for a given R the rate experimentally depends upon the nature of the species on the surface.[46−48] For example, Gutierrez and Henglein showed that a saturation surface coverage of I^- anions (at 10 μM KI) on colloidal Ag increased the plasmon width by about a factor of 2. In larger particles, radiative Mie scattering begins to dominate the bulk and surface nonradiative relaxation processes. This is the case for the coupled system of two nearly touching 30-nm Ag nanocrystals, where a huge SERS effect is seen in the junction. Here it has been shown that the excited Ag electronic polarization concentrates on the metallic surface in the junction, in contrast to single particles where the excited polarization is a uniform volume polarization inside the nanocrystal.[49] Such dimers should show significant decarboxylation of the stabilizing citrate anion in the junction.

Thus, the quantum yield of Ag hot-carrier interaction with surface molecules can be quite high, possibly with transient capture of the excited carrier and the resulting very-strong (first-layer) SERS.[50] A high yield for photochemistry depends upon a fast subsequent rate of irreversible reaction that can compete with return of the hot carrier to the nanocrystal. With adsorbed citrate in RWB, we observed a net yield of about 1%, compared to the Mie Scattering rate. In an electrochemical photoemission

experiment, a yield of 5% has been reported for the creation of a thermalized aqueous solvated electron, followed by irreversible CO_2 reduction.[51] In this situation, the photoexcited electron tunnels through adsorbed surface species to reach the solvent. All in all, "hot-electron" processes are a novel type of metal-based photochemistry that need to be explored further.

Conclusions

Photocharged, citrate-stabilized Ag nanocrystals decay through a thermal electrochemical charge-transfer process described quantitatively by the Butler−Volmer equation, without effects due to mass transport. The kinetics are quite slow with large activation energies, apparently due to the citrate passivation layer. Under continuous low-intensity plasmon excitation, the particles reach a steady-state photovoltage shift when the photochemical charging rate is equal to the electrochemical discharging rate. We discuss the quantum yield and systematics of charge-transfer photochemistry resulting from Ag plasmon irradiation. The quantum yield can be high for well-formed nanocrystals if the surface adsorbed molecular species undergoes a fast irreversible chemical process upon capture of the hot electron.

Acknowledgment. We thank Radoslav Adzic for valuable comments on an earlier draft of this manuscript. This work has been supported primarily by the DOE Basic Energy Sciences FG02-98ER14861 and by an AFOSR MURI. We have used characterization facilities supported by the Columbia NSF Nanocenter CHE-010110655, by the New York Office of Science, Technology and Academic Research (NYSTAR), and the Columbia NSF MRSEC materials center DMR 02123547.

Supporting Information Available: A cyclic voltammogram of a silver particle electrode in a solution of silver nitrate and sodium citrate. This material is available free of charge via the Internet at http://pubs.acs.org.

References and Notes

(1) Zhdanov, V. P.; Hagglund, C.; Kasemo, B. *Surf. Sci. Lett*. **2005**, *599*, L72.

(2) Douketis, C.; Haslett, T. L.; Shalaev, V. M.; Wang, Z.; Moskovits, M. *Physica A* **1994**, *207*, 352.

(3) Nolle, E. L.; Shchelev, Ya, M. *Tech. Phys. Lett.* **2004**, *30*, 304.

(4) Lemann, J.; Merschdorf, M.; Pfeiffer, W.; Thon, A.; Voll, S.; Gerber, G. *J. Chem. Phys*. **2000**, *112*, 5428.

(5) Kennerknecht, C.; Hovel, H.; Merschdorf, M.; Voll, S.; Pfeiffer, W. *Appl. Phys. B* **2001**, *73*, 425.

(6) Merschdorf, M.; Pfeiffer, W.; Thon, A.; Voll, S.; Gerber, G. *Appl. Phys. A* **2000**, *71*, 547.

(7) Link, S.; El-Sayed, M.A. *J. Phys. Chem. B* **1999**, *103*, 8410.

(8) A broad-band short pulse is required to excite the formal zero-order plasmon excitation. When using narrow-band CW excitation, the spectral band width is not present to excite the formal plasmon; instead, the decay products are directly excited. This is also the case for illumination by low-intensity incoherent light. Each case (broad and narrow band) should produce "hot holes" available for photochemistry; however, the yields may be different.

(9) Liau, Y-H;, Unterreiner, A. N.; Chang, Q;, Scherer, N. F. *J. Phys. Chem. B* **2001**, *105*, 2135.

(10) Hu, M.; Hartland, G. V. *J. Phys. Chem. B* **2002**, *106*, 7029.

(11) Hodak, J. H.; Martini, I.; Hartland, G. V. *J. Phys. Chem. B* **1998**, *102*, 6958.

(12) Maillard, M.; Huang, P.; Brus, L. *Nano Lett.* **2003**, *3*, 1611.

(13) Jin, R.; Cao, Y. C.; Hao, E.; Metraux, G. S.; Schatz, G. C.; Mirkin, C. A. *Nature* **2003**, *425*, 487.

(14) Jin, R.; Cao, Y. W.; Mirkin, C. A.; Kelly, K. L.; Schatz, G. C.; Zheng, J. G. *Science* **2001**, *294*, 1901.

(15) Bastys, V.; Pastoriza-Santos, I.; Rodriguez-Gonzalez, B.; Vaisnoras, R.; Liz-Marzan, L. M. *Adv. Funct. Mater*. **2006**, *16*, 766.

(16) Kyung Kim. S. Lee, Kwan Kim, *J. Phys. Chem. B* **2004**, *108*, 9216.

(17) Sun, Y.; Xia, Y. *Adv. Mater*. **2003**, *15*, 695.

(18) Jia, H.; Zeng, J.; Song, W.; An, J.; Zhao, B. *Thin Solid Films* **2006**, *496*, 281.

(19) Barker, G. *Electrochem. Acta*. **1968**, *13*, 1221.

(20) Sass, J.; Sen, R.; Meyer, E.; Gerischer, H. *Surf. Sci*. **1974**, *44*, 515.

(21) Funtikov, A.; Sigalev, S.; Kazarinov, K. *J. Electroanal. Chem*. **1987**, *228*, 197.

(22) Zheng, J.; Lu, T.; Cotton, T.; Chumanov, G. *J. Phys. Chem B* **1999**, *103*, 6567.

(23) Pursell, D.; Dai, H. L. *J. Phys. Chem B* **2006**, *110*, 10374.

(24) Redmond, P.L.; Wu, X.; Brus, L.E. *J. Phys. Chem. C* **2007** ASAP.

(25) Budac, D.; Wan, P. *J. Photochem. Photobiol., A* **1992**, *67*, 135.

(26) Garewood, R.; Scott, C.; Weedon, B. *Chem. Commun*. **1965**, *14*.

(27) Kraeutler, B.; Bard, A. J. *J. Am. Chem. Soc*. **1977**, *99*, 7729.

(28) Kraeutler, B.; Bard, A. J. *J. Am. Chem. Soc*. **1978**, *100*, 5985.

(29) This wavelength was chosen to be near the plasmon resonance of the particles. Photocurrent was also observed at 457 nm, 514 nm, and greatly reduced at 633 nm laser-light illumination consistent with the broad plasmon absorption of the particle electrode.

(30) Lee, P. C.; Meisel, D. *J. Phys. Chem*. **1982**, *86*, 3391.

(31) Henglein, A.; Giersig, M. *J. Phys. Chem B*, **1999**, *103*, 9533

(32) Henglein, A.; Lillie, J. *J. Am. Chem. Soc*. **1981**, *103*, 1059.

(33) Here we have assumed a single rate-determining step for the multistep hydrogen reduction in accordance with refs 32 and 35.

(34) dV/dt was found by monitoring the potential as the electrode discharged as a function of time. dV/dt was taken as the instantaneous rate of the decay at each point in time (i.e., the tangent of the decay at time t).

(35) Eberhardt, D.; Santos, E.; Schmickler, W. *J. Electroanal. Chem*. **1999**, *461*, 76.

(36) Here it is important to remember that the gold wire is a *pseudo-reference* electrode whose potential may shift in different solutions (but remains constant for a given solution). The gold wire shifts ∼20 mV in solution with this concentration of silver nitrate compared to the solution without silver nitrate.

(37) Jaffrezic-Renault, N.; Revel, G.; Cachet, C.; Froment, M.; Wiart, R. *J. Electroanal. Chem*. **1983**, *146*, 343.

(38) Grishko, V. I.; Duley, W. W.; Gu, Z. H.; Fahidy, T. Z. *Electrochim. Acta* **2001**, *47*, 643−650.

(39) Wee, L. M.; Li, L. *Appl. Surf. Sci.* **2005**, *247*, 285−293.

(40) Redmond, P. L.; Walter, E. C.; Brus, L. E. *J. Phys. Chem. B* **2006**, *110*, 25158.

(41) Redmond, P.L.; Wu, X.; Brus, L. *J. Phys. Chem. C*, in press.

(42) The experimental capacitance would not change, but the theoretical capacitance would require an N that represents the total number of particles in contact with the ITO.

(43) This assumption would not change the experimental or theoretical capacitance. But it would require that the few active particles experience a larger photovoltage shift. For example, if only 10% of the particles are active, those particles would have to experience a −100 mV shift for the ensemble measurement to show a −50 mV potential shift. As before, this calculation is done by balancing the discharging rate (defined by the Butler−Volmer equation) with the charging rate (J). However, in this case the charging current is attributed to a few particles, which then have a larger potential shift. Every particle (photoactive and photoinactive), contributes to the electrochemical discharging rate.

(44) Gutierrez, M.; Henglein, A. *J. Phys. Chem.* **1993**, *97*, 11368.

(45) Bauer, C.; Abid, J.; Fermin, D.; Girault, H. *J. Chem. Phys.* **2004**, *120*, 9302.

(46) Mulvaney, P. *Langmuir* **1996**, *12*, 788.

(47) Kreibig, U.; Volmer, M. *Optical Properties of Metal Clusters*; Springer-Verlag: New York, 1995.

(48) Charle, K.: Schatze, W.; Winter, B.; *Z. Phys. D* **1989**, *12*, 471

(49) Jiang, J.; Bosnick, K.; Malliard, M.; Brus L.; *J. Phys. Chem B* **2003**, *107*, 9964

(50) Otto, A. *J. Raman Spectrosc*. **2005**, *36*, 497.

(51) Fedurco, M.; Shklover, V.; Augustynski, J. *J. Phys. Chem. B* **1997**, *101*, 5158.